New geomorphological and chronological constraints for glacial deposits in the Rivoli-Avigliana end-moraine system and the lower Susa Valley (Western Alps, NW Italy)

New geomorphological and chronological constraints for glacial deposits in the Rivoli-Avigliana end-moraine system and the lower Susa Valley (Western Alps, NW Italy)

Autori: Ivy-Ochs, Susan*; Lucchesi, Stefania; Baggio, Paolo; Fioraso, Gianfranco; Gianotti, Franco; Monegato, Giovanni; Graf, Angela A.; Akçar, Naki; Christl, Marcus; Carraro, Francesco; Forno, Maria Gabriella; Schlüchter, Christian

JOURNAL OF QUATERNARY SCIENCE 2018 Volume 33 p.550-562

Digital Object Identifier (DOI): 10.1002/jqs.3034

Versione pubblicata: http://www.interscience.wiley.com/jpages/0267-8179

Parole Chiave: Cosmogenic10Be; European Alps; Exposure dating; Last Glacial Maximum; Moraine amphitheatre

Abstract:

Our new dataset from the Rivoli-Avigliana end-moraine system, the westernmost amphitheatre of the Italian Alps, provides an important step towards understanding foreland-reaching glaciations before and during the Last Glacial Maximum (LGM) in the Western Alps. 10Be data from six boulders in pre-LGM deposits gave ages between 26.82.1 and 41.21.9 ka. Based on morphological and pedological data, we interpret the oldest age as a minimum age for the glacier advance(s). 10Be results suggest that the LGM occurred in two major steps. During the first at 24.01.5 ka, several ridges were constructed demonstrating oscillation of the Dora Riparia glacier snout at the maximum position. Our data demonstrate a significantly larger LGM extent in the Rivoli- Avigliana amphitheatre than shown on previous maps. The maximum advance was followed by a short re-advance of the glacier at 19.60.9 ka, as recorded by 10Be ages from boulders in lateral positions along the lower Susa Valley. The maximum ice surface during the LGM was at 1000–920m a.s.l. in the final reach of the valley (560– 620m of elevation above the alluvial plain) and at 620–340m a.s.l. at the continuous moraines in the amphitheatre.

Abbreviations

AMS accelerator mass spectrometry

ELA equilibrium line altitude

LGM Last Glacial Maximum

MIS Marine Isotope Stage

Introduction

Along the southern fringe of the European Alps, several end-moraine systems were built by Pleistocene glacier piedmont lobes flowing out of the major trunk valleys (Fig. 1). Their stratigraphic reconstruction allowed, since the late 19th century (e.g. Gastaldi, 1872), the recognition of several different glacier advances, which were subsequently assigned to glaciations based initially on the classic fourfold chronostratigraphic subdivision of Penck and Brückner (1909). As chronological data became available it became clear that in each of the major systems a distinctly different number of glacial units was preserved (Bini, 1997). Orography, climate and tectonic factors acted as drivers in dissimilar ways at each system and during each glaciation. The overall arcuate E–W orientation of the southern Alpine fringe with respect to atmospheric circulation patterns may have led to extreme differences in precipitation rates across the Alps [models for the Last Glacial Maximum (LGM) by Florineth and Schlüchter, 2000; Luetscher et al., 2015] and thus equilibrium line altitude (ELA) depression (Kuhlemann et al., 2008; Federici et al., 2012; Monegato, 2012). By contrast, Quaternary tectonic activity in the Western and Central Alps, which are affected by

marked isostatic uplift (Champagnac et al., 2007; Scardia et al., 2012; Sternai et al., 2012; Mey et al., 2016; Nocquet et al., 2016), was starkly different from that in the eastern Southern Alps, which are dominated by thrusting and foreland subsidence (Galadini et al., 2005; Scardia et al., 2015). In this framework, reliable age assessments for the deposits of the several end-moraine systems have so far been achieved only for the late Matuyama glaciation, through magnetostratigraphic analyses (Carraro et al., 1991; Scardia et al., 2015), and for the LGM at Tagliamento (Monegato et al., 2007), Garda (Ravazzi et al., 2014; Monegato et al., 2017), Ivrea (Gianotti et al., 2008, 2015), and in the Gesso system in the Maritime Alps (Federici et al., 2012, 2016). We follow Clark et al. (2009), Shakun and Carlson (2010), and Hughes and Gibbard (2015) in their definition of the global LGM as being during Marine Isotope Stage 2 (MIS2) (Lambeck et al., 2014).

The present work focuses on the Rivoli-Avigliana end-moraine system, which is the westernmost system of the Italian piedmont plain (Po Plain). The end-moraine system is located in the lower reach of the Susa Valley as well as downstream of the valley outlet where a moraine amphitheatre built-up over numerous glacier advances. The primary goal of this study is to use new field survey evidence and cosmogenic 10Be exposure dating to find a clear solution for the attribution of moraines in the amphitheatre to the LGM. The data then serve as the starting point for comparing the timing and extents of foreland-reaching lobes across the Alps. Such a comparison is crucial for reconstructing precipitation patterns during the LGM, which were markedly different from today's (Florineth and Schlüchter, 2000; Kuhlemann et al., 2008; Hofer et al., 2012; Luetscher et al., 2015; Ludwig et al., 2016; Monegato et al., 2017).

In this work, we present a new 10Be dataset from erratic boulders located on the crests of moraines previously referred to the Riss and Würm glaciations (Bonsignore et al., 1969; Petrucci, 1970) or to distinct glacier advances in the Late Pleistocene (Balestro et al., 2009a) (see also below). This is a first attempt to correlate the deposits in the lower valley with those of the end-moraine system. The results led to a new stratigraphic interpretation of the ice extent in the Dora Riparia catchment at the time of the global LGM. We show that the LGM extent was notably greater than shown in previous interpretations. Our data yield elements for a broad correlation to the other glaciated systems of the Western Alps, and fills the gap between sites to the east and west that have isotopic dating control. These include the Gesso Valley system in the Maritime Alps (Federici et al., 2012, 2016) and the Ivrea end-moraine system (Gianotti et al., 2008, 2015) where cosmogenic 10Be dating was applied (Fig. 1). Further comparison is allowed with the Tagliamento and Garda systems, which have been dated with radiocarbon (Monegato et al., 2007, 2017).

Geological setting and previous work

The catchment of the Dora Riparia River covers 1050 km2. Mean elevation is 1450 m a.s.l., with a maximum at 3612 m a.s.l. (Punta Roncia), and many plateaus up to 2500–3000 m a.s.l. The river lies in a W–E orientated 65-km-long trunk valley, which joins the roughly N–S trending tributary Cenischia Valley at the city of Susa. The valley bottom of the latter has a lower elevation and the junction with the Susa Valley forced the Dora Riparia River into a deep gorge. Downstream, the valley widens with only small side tributary valleys until the outlet in the Po Plain. The 150 km2 Rivoli-Avigliana end-moraine system encloses the outlet of the valley (Fig. 2). The Dora Riparia River flows through the inner plain of the end-moraine system and the outwash plain to join the Po River in Turin, at 215 m a.s.l.

The Dora Riparia River carves into a continental and oceanic composite nappe system which belongs to the Penninic domain and includes: (i) the ophiolitic Piedmont Zone, with Mesozoic carbonate to terrigenous metasediment (calcschists) and preserved oceanic crust units (Chenaillet Complex) and mantle peridotite (Lanzo Complex); and (ii) the palaeo-European continental basement nappes (Ambin and Dora Maira) and related Mesozoic metasediment covers (Carraro et al., 2002; Polino et al., 2002; Balestro et al., 2009a). The most common lithologies in the catchment are (in order of abundance) calc- and micaschist, gneiss, prasinite, gabbro, eclogite, serpentinite, peridotite and locally some carbonates. The lower reach of the

valley also includes Pliocene to Lower Pleistocene continental sequences ('Villafranchian' Auct.; Balestro et al., 2009a).

The Susa Valley is bordered at its western and eastern ends by two regional fault systems: (i) a longitudinal fault system (Barféty et al., 1996; Sue and Tricart, 2003), characterized by an early phase of normal activity and subsequent right-lateral reactivation during the Pliocene, and (ii) the Canavese Line and Col del Lys − Trana Deformation Zone, with dextral transtensive displacement, active since the Late Oligocene, and a last Plio-Pleistocene reactivation, documented in the lower Susa Valley, which involved pre-glacial continental successions (Balestro et al., 2009b; Perrone et al., 2015, 2010). A transverse fault system (Barféty et al., 1996; Sue and Tricart, 2003) lies between these two N–S fault systems, corresponding to NE–SW trending normal faults with evidence of left-lateral reactivation.

The study area has been investigated since the second half of the 19th century (Sacco, 1887) and was mapped in the first edition of the Italian Geological Map (Mattirolo et al., 1910; Franchi et al., 1925), in which three main glacial units related to the 'Mindel', 'Riss' and 'Würm' glaciations were defined according to the chronostratigraphic scheme of Penck and Brückner (1909). Updated geological maps (Bonsignore et al., 1969; Petrucci, 1970) allowed re-interpretation of the stratigraphy of the end-moraine system. At that time, most of the glacial deposits in the amphitheatre were attributed to the 'Riss' glaciation (Fig. 3A). Without chronological control, and due to the close stacking of numerous moraines, age assignment remained ambiguous and varied between maps of different generations. In recent decades, the lower reach of the Susa Valley has been surveyed to complete the new Italian Geological Map at the scale 1: 50 000, namely the 'Susa' (Cadoppi et al., 2002) and 'Torino Ovest' (Balestro et al., 2009a) sheets. The stratigraphic subdivision was based mainly on morphostratigraphic and pedostratigraphic criteria, with few chronological constraints (Charrier and Peretti, 1973, 1975; Finsinger et al., 2006). In detail, five units were distinguished in the moraine amphitheatre (Balestro et al., 2009a) (Fig. 3B): (i) two units of highly weathered glacial deposits forming topographically smoothed moraines probably related to the Middle Pleistocene − San Gillio synthem and Bennale synthem; (ii) and three units of little weathered glacial deposits forming a huge set of ridges related to the Late Pleistocene − Frassinere and Magnoletto synthem, and Crescentino subsynthem. The widest Frassinere synthem was subdivided into two units referred to the early and to the late Upper Pleistocene, respectively: the Cresta Grande subsynthem, corresponding to the highest but not entirely continuous moraines, and the more internal Col Giansesco subsynthem a set of continuous moraines.

Methods

Landform characterization and glacial unit assignment

Starting from the recent geological maps (Cadoppi et al., 2002; Balestro et al., 2009a), the stratigraphy and geomorphology of the Rivoli-Avigliana end-moraine system were re-interpreted based on new field survey, aerial photos, subsurface data and construction of cross-sections. Moreover, a high-resolution topographic map with 2-m spaced contour lines, generated from the digital elevation model with grid cell size of 5 m, was also used for the geomorphological mapping. A new stratigraphic subdivision was obtained using morphostratigraphic criteria (Gibbons et al., 1984). The continuity of the moraines and related landforms allow a high degree of accuracy in tracing stratigraphic limits over large areas of the amphitheatre (Rose and Menzies, 1996). Each moraine or group of similar moraines was initially regarded as separated from the others and then grouped according to geomorphological and sedimentary characteristics, including degree of weathering assessed using Munsell colour charts and details of the soil profiles. Final age assignment is based on cosmogenic 10Be exposure ages in concert with morphological evidence.

Cosmogenic 10Be surface exposure dating

Samples were collected from boulders on moraines in the amphitheatre and on both flanks of the lower Susa Valley (Fig. 4). Geographical and morphological details, as well as age calculation parameters, are given in Table 1. Photos of several sampled boulders are shown in Fig. 5. Samples for 10Be analysis were prepared from quartz mineral separates following the procedures of Ivy-Ochs et al. (2006). 10Be/9Be ratios were measured with accelerator mass spectrometry (AMS) with the 6-MV tandem accelerator (Christl et al., 2013) at the Laboratory of Ion Beam Physics at ETH Zürich. Samples were originally measured against the in-house standard S555 (Graf, 2008). Values listed in Table 1 have been corrected to new standard vales and are now consistent with the 07KNSTD standard (Nishiizumi et al., 2007). A blank correction of $2.56 \pm 0.13 \times 10{-}14$ was made. To calculate exposure ages we use the CRONUS-Earth online calculator (Balco et al., 2008) version 2.2 with a spallation production rate at sea level and high latitude of 3.93 ± 0.19 10Be atom gquartz−1 a−1 'NENA' (Balco et al., 2009) with 'St' scaling (Stone, 2000). This production rate agrees well with results from the Chironico landslide in Ticino, Switzerland (Claude et al., 2014), and the global averaged 10Be production rates recently published by Heyman (2014) and Borchers et al. (2016). We used a boulder surface erosion rate of 1 mm ka−1. No correction for snow cover was made. Stated uncertainties are analytical only. Radiocarbon dates are calibrated with Oxcal 4.2.

Geomorphology and age of the glacial units

The Rivoli-Avigliana end-moraine system exhibits an elongate E–W geometry and is strongly asymmetrical in plan view (Fig. 4). This configuration originated as ice advancing out of the Susa Valley was constrained along the left-hand side by a bedrock ridge that extends 8 km farther to the east than the bedrock on the right-hand side of the valley outlet. As a result, the amphitheatre shows a large southern and south-eastern sector with numerous well-separated moraines. In contrast, the northern sector is narrow with closely spaced and discontinuous moraines resting on the steep slopes of the Rocca della Sella-Musiné mountain reliefs (M. Musiné on Fig. 4). At the valley outlet the glacier split into two lobes as it abutted against the Moncuni inselberg, resulting in the formation of a bi-lobate end moraine system. In detail, a main (13 km long and 7–11 km wide) moraine arc extends with a W–E trend, encircles a 23 km2 inner alluvial plain crossed by the Dora Riparia River and ends with a large frontal sector between Rivoli and Alpignano. In the south-western sector, a second much less extensive moraine amphitheatre (6 km long and 4 km wide), with an NNW–SSE trend, encircles the two Avigliana lakes (Lago Grande and Lago Piccolo) and closes with a set of terminal moraines at Trana.

Considering the distribution of glacial deposits in the Rivoli-Avigliana end-moraine system and in the lower Susa Valley, several moraines were distinguished. They can be referred to glacial stadials of the same glaciation or to distinct glaciations, on the basis of pedostratigraphic data (Balestro et al., 2009a) and the new surface exposure dates presented in this work, with particular attention to the LGM (Fig. 3C). Hence, the recognized moraines were grouped into three different sets of deposits and related forms (Figs 4 and 6), namely: (i) the pre-LGM units made up of the most external moraines, (ii) the LGM unit related to the maximum advance corresponding to the more external ridges of the little-weathered moraines and (iii) the LGM recessional units (including all the ridges in more internal positions than the LGM maximum).

Pre-LGM units

Pre-LGM glacial deposits are found in the outermost sector of the Rivoli-Avigliana amphitheatre as well as on the flanks of the lower Susa Valley (Figs 4 and 6). Pre-LGM units constitute about 50% of the total area of the moraine relief and include the Cresta Grande moraine complex.

Pre-LGM units in the amphitheatre

The more external moraines (the Bennale synthem of Balestro et al., 2009a) are markedly weathered (2.5YR-5YR hues) with relatively flat crests. The pre-LGM moraines are mostly frontal moraines, although they enclose several lateral moraines (Fig. 4). They are especially extensive on the right side, where there are two distinct groups of ridges at Villarbasse (about 370 m a.s.l.). On the left side, a discontinuous belt of low moraines can be followed from north of Caselette, at the base of the eastern slopes of Mount Musinè, to San Gillio and Pianezza. External to these moraines lie the outwash terraces, which are widely covered by decimetre- to metre-thick loess deposits. These terraces display up to 10-m-thick, well-developed soils (10R to 5YR hues), which contain cemented horizons and clasts that are often completely weathered. It is likely that these deposits can be attributed to the Middle Pleistocene.

The Cresta Grande moraines, the most extensive moraines in the amphitheatre, are in a slightly more internal position than the deposits described above, close to Rivoli (Fig. 4). The ridges are the highest moraines (40 m high) in the SE sector of the amphitheatre. The sediments show only moderate weathering, evidenced by the widespread presence of a soil C-horizon with hue 10YR on the crests. Remnants of truncated B-horizons reaching hue 7.5YR are also encountered. Weathering cortexes on clasts are <1 mm. These moraines are considered of pre-LGM age as they are perceptibly more weathered than the moraines further inboard that we attribute to the LGM (see below). Nevertheless, unequivocal data for age attribution are lacking. In the south-western part of the system, these moraines partially dammed the outlet in the Po Plain of the Sangone Valley, and forced the Sangone River to flow close to the slope of Mount Pietraborga. A single large boulder from the pre-LGM moraines in the southern sector was located to exposure date. RE1b lies on a ridge (463 m a.s.l.) between the villages of Trana and Reano. As shown in Fig. 4, the boulder lies on a ridge that is external to the Cresta Grande moraine, which itself is classified as pre-LGM. The ridge on which RE1b is located arcs to the north and is about 5 m higher in elevation than the Trana LGM moraines (see also below). In addition, the Moncuni bedrock hill separates the RE1b ridge from the ridges of the Avigliana lakes LGM lobe. We consider the exposure age of RE1b, 26.8 ± 2.1 ka, to be a minimum age. Based on the geomorphological relationships of the ridges, the boulder was deposited during a pre-LGM glaciation and may have been later exhumed and/or rotated.

On the left-hand side of the amphitheatre lie the impressive moraines of Rubiana (680–725 m a.s.l.). Based on topographic relationships and a plausible reconstructed ice surface, the outermost Rubiana moraines are correlated with the Cresta Grande moraines. The outer Rubiana moraine dammed the Torrent Messa causing the formation of an ice-marginal lake in the tributary valley. Here, charcoal fragments were found in the lower part of a glacial succession composed of glaciolacustrine deposits covered by subglacial till, which forms the base of this moraine. This succession appears to be continuous, as inferred by the lack of a palaeosol. The obtained radiocarbon date for the charcoal was beyond the method (>45 14C ka bp; LTL12084A, CEDAD Lab, Università del Salento), confirming the chronological attribution of the outer Rubiana moraines to pre-LGM glaciations.

Pre-LGM units in the lower Susa Valley

Within the lower Susa Valley, glacial deposits are found scattered above 1000 m a.s.l. and defined as ‘skeletal till’ by Cadoppi et al. (2002). Boulder accumulations are found associated with rarely preserved subglacial tills. In accordance with their elevation and the marked morphological modification, these

deposits on the steep valley flanks are regarded as having been deposited during glaciations before the LGM.

Three boulders from the Truc Bruje − Combe site, on left side of the lower Susa Valley at ca. 1135 m a.s.l., were sampled (Fig. 4). The exposure ages of CO1 and CO2a are 41.2 ± 1.9 and 34.1 ± 1.5 ka, respectively. For the two samples from boulder CO3, we obtained ages of 29.0 ± 1.6 ka (CO3a) and 27.9 ± 1.1 ka (CO3b), which yields a weighted mean of 28.3 ± 0.9 ka. All three boulders are located on an interfluve with a gentle morphology (Fig. 6A), where a fairly well-developed Quaternary cover mantles the bedrock without any relict morphological evidence. Their elevation (ca. 1135 m a.s.l.) places them higher than the sharp-crested lateral moraines located at about 1000 m a.s.l., which are ascribed to the LGM. They therefore were deposited during glacier advances before the LGM and the ages must be considered as minimum ages. Both CO1 and CO3 are highly weathered and spalling of large flakes or post-depositional exhumation may have occurred. These boulders are located in a settled area, where anthropogenic impact cannot be ruled out. CO2a has numerous angular surfaces (Fig. 5B), suggesting it may have been quarried for the highly resistant quartzite (cf. Akçar et al., 2011). The maximum age of the three boulders, 41.2 ± 1.9 ka (CO1), thus provides a minimum age for deposition of the glacial sediments.

Along the right side of the valley, we sampled two boulders (SM1, SM3) in a very different setting than CO1-3. In the small tributary Procchio Valley, the remnants of ice-marginal deposits are located just south of the village of Bennale (Fig. 4). They lie at 1065 m a.s.l., i.e. 60 m lower than the Truc Bruje − Combe boulders but 3 km downstream, so the elevation along the longitudinal profile of the palaeoglacier surface is comparable (Fig. 7B). Two of the many boulders (most too small to be suitable for dating) preserved along the lateral moraine crest were sampled. Boulders SM1 and SM3 yielded ages of 30.6 ± 1.8 and 27.2 ± 1.3 ka, respectively. Based on site elevation, they are attributed to a pre-LGM advance of the Dora Riparia glacier. No evidence of a former local glacier was found at the Procchio Valley head, in accordance with the fact that the elevation of headwaters of this small basin is too low for hosting local glaciers (max. 1300 m a.s.l.).

LGM units

LGM units in the amphitheatre

A prominent complex of well-developed moraines (LGM A-unit in the map, Fig. 4) is located internal to the Cresta Grande moraines. In the proximal sector, their crests reach similar heights (around the Lago Grande and at Rubiana) to those of Cresta Grande (ca. 40 m), but the elevation of the crests drops rapidly downstream to a few tens of metres lower than the Cresta Grande crests west of Rivoli. Two moraine ridges have been grouped into this unit. The external ridge shows a similar pattern to the Cresta Grande moraines, as they are continuous only from the Moncuni hill to west of Rivoli and on the right side of the Avigliana lobe. These moraines are discontinuous and breached at several points. The internal ridge is, in contrast, more continuous in both frontal sectors (Alpignano and Trana). Glacial deposits of both these ridges bear little evidence of weathering, with soil development reaching 7.5–10YR hue index. Normally only a thin C-horizon with a 5Y olive colour hue is preserved on the crests. As they are the most external of the little-weathered moraines, these are ascribed to the maximum expansion of the glacier during the LGM.

The two boulders of Trana (TR1 and TR2) come from the lobe in the south-western sector of the amphitheatre, not far from RE1b, but in a markedly different morphological context. Both TR1 and TR2 rest on the western slope of the Moncuni hill (641 m a.s.l.), a high rocky inselberg made of serpentinites and

peridotites, which forms the left side of the moraine complex encircling the Avigliana Lakes. In contrast, RE1b lies on the right side of the latero-frontal complex of the Rivoli lobe (Fig. 4). TR1 lies on a small terrace forming a break in the steep slope of the Moncuni hill at 480 m a.s.l. Its exposure age is 24.0 ± 1.5 ka. TR2 is located 250 m north-west of TR1 and at a comparable elevation (470 m), but has a slightly younger exposure age, 20.9 ± 2.1 ka. We interpret the older age to represent the time of moraine formation, while the younger age may relate to later exhumation or more probably toppling of the boulder, given the position of TR2 on a steep slope.

Late LGM units in the amphitheatre

Inside the major ridges we attribute to the LGM, several moraines with crests at lower elevation are preserved (LGM B-unit on the map, Fig. 4). Four major morphological sub-units, which are continuous across the whole Rivoli-Avigliana amphitheatre, can be distinguished. These moraines are generally not very high (a few tens of metres at most) and of progressively decreasing heights but with sharp crests. They are often coupled with wide kame terraces on their inner flanks. Moreover, the various ridges are separated by extensive elongated depressions filled with glaciolacustrine and glaciofluvial deposits. Glacial deposits are weakly weathered, similar to the LGM A-unit moraines. Because of their inner position, these moraines are attributed to minor glacier re-advances or stillstands similar to the LGM stadials of the northern Alpine forelands (Ivy-Ochs, 2015 and references therein). In the south-west sector, they encircle and separate the Avigliana lakes. The oldest radiocarbon age from identifiable macrofossils at 909-cm depth from a sediment core drilled in the Lago Piccolo (location indicated on Figs 3 and 5C) is 14 930 ± 80 14C a bp (18 365–17 926 cal a bp) (Finsinger et al., 2006; Larocque and Finsinger, 2008). Sediment from the bottom of the core (1492 cm) up to just above the dated horizon (900-cm depth) comprises blue–grey silt and sand with angular stones, compatible with a glacier pinned at the moraine that bounds the lake to the north. The calibrated radiocarbon date provides a minimum age for that moraine, which lies internal to the moraine dated with boulders TR1 and TR2.

LGM and late-LGM units on the lower Susa Valley flanks

Three boulders from LGM positions in the lower Susa Valley were dated (CO4, SM4, MA1a). In detail, CO4 is located on one of the highest LGM maximum lateral moraines, while SM4 and MA1a are found at slightly lower elevation (Fig. 6A). The tributary Gravio Valley hosted a lateral lobe of the Dora Riparia glacier, as evidenced by the presence of moraines that trend into the valleys on the left side (Fig. 4). Nevertheless, the distribution of other, local moraines and glacial deposits suggests that the front of the Gravio tributary glacier flowed down at very low altitude during withdrawal of the trunk glacier. The large CO4 erratic boulder is located on the flat crest of a well-formed moraine of the trunk glacier, along the right side of the Gravio Valley at 925 m a.s.l. (Fig. 6). Its exposure age, 17.8 ± 2.4 ka, is younger than the likely age of moraine deposition based on its location, which indicates formation during the LGM. The huge size of boulder CO4 and its position on a broad crest obviates post-depositional movement or exhumation (Fig. 5D). The slightly younger age may be due to exfoliation of the top surface.

Within the lower Susa Valley, we dated two boulders that lie on ice-marginal positions on the valley flanks. They rest at lower elevations than the boulders discussed above (Fig. 4). MA1a, whose exposure age is 19.6 ± 0.9 ka, is located at 622 m a.s.l. on a bedrock ridge which separates the left side of the valley from the tributary Gravio Valley. SM4 is located at 821 m a.s.l. on the right side of the valley, 1 km upstream of boulder MA1a. It is a partially smoothed large block (350 m3) resting on a steep slope. The fact that its base

is well embedded into subglacial till, as clearly visible in outcrop, suggests the absence of post-depositional movement of the block. Its exposure age is 19.5 ± 2.0 ka. Considering their low elevations, both MA1a and SM4 were deposited during LGM recessional stages (LGM B-unit in Fig. 4). In the lower reach of the valley close to Villar Dora (Fig. 4), two radiocarbon dates came from lacustrine deposits containing peat layers close to the surface (Charrier and Peretti, 1973, 1975): a wood fragment of pine yielded an age of 10 000 ± 75 14C a bp (11 801–11 244 cal a bp) and bulk sample from a peat layer gave an age of 7780 ± 100 14C a bp (8976–8391 cal a bp).

Stratigraphy of the Rivoli-Avigliana end-moraine system and lower Susa Valley

The updated stratigraphical and geomorphological analyses coupled with the 10Be data provide elements for revision of the chronostratigraphic architecture of the Rivoli-Avigliana end-moraine system (Figs 3C and 4) and the related deposits preserved in the lower Susa Valley (Cadoppi et al., 2002; Balestro et al., 2009a).

The pre-LGM moraines include the highest ridge (Cresta Grande) as well as further outboard moraines. No 10Be dates are available from the latter deposits. These older units have been extensively modified by colluvial processes and are characterized by mature soils (Cadoppi et al., 2002; Balestro et al., 2009a). For many of these deposits, the degree of soil development and erosion are consistent with deposition during Middle Pleistocene glacier advances, as discussed for the nearby Ivrea end-moraine system (Gianotti et al., 2015). 10Be exposure ages for six erratic blocks (CO1, CO2a, CO3a/CO3b, SM1, SM3 and RE1b) from deposits external to and/or higher than the LGM moraines range from 26.8 ± 2.1 to 41.2 ± 1.9 ka. These boulders are all clearly associated with pre-LGM glacial deposits. Considering their morphostratigraphical position and elevation, they may be attributed to the Cresta Grande units. The oldest obtained age (CO1: 41.2 ± 1.9 ka) gives a minimum age for deposition of these units, but they may have been deposited much earlier (cf. Graf et al., 2015). Conversely, it cannot be ruled out that the less weathered pre-LGM units (Cresta Grande complex) were deposited during MIS3 or MIS4 as shown for example in the Pyrenees (Delmas, 2015).

Several stacked moraines located internal to the Cresta Grande and characterized by immature soils are assigned to the LGM. The boulders of Trana (TR1 and TR2) locate the LGM extent along the western side of the Moncuni hill (Fig. 4). The outermost LGM units are continuous in the amphitheatre, except at the northern flank, and can be traced along the entire end-moraine system. Based on re-assessment of morphological position and our 10Be dates, we propose a new larger LGM extent at Rivoli-Avigliana (compare Fig. 3A, 3B and 3C). The maximum glacier extent during the LGM was attained around 24.0 ± 1.5 ka (TR1).

Late LGM climate oscillations are recorded by the series of low-elevation (400–350 m a.s.l.) nested moraines that encircle the Avigliana lakes and form a continuous belt inside the main LGM moraine system. At Lago Piccolo, the oldest age gained from lake sediments, 18 365–17 926 cal a bp (Larocque and Finsinger, 2008), is a minimum for ice-free conditions. The boulders of the lower reach of the valley located below the extent of the LGM maximum lateral moraines (MA1a, SM4) can be ascribed to the late stages of the LGM, just before the onset of rapid downwasting. The boulder ages 19.5 ± 2.0 ka (SM4) and 19.6 ± 0.9 ka (MA1a) pinpoint the last moment of ice occupation in the lower Susa Valley, with the glacier front still in the amphitheatre.

Discussion

These new chronological data are useful for improving the regional stratigraphic framework of the Alpine LGM. The Western Alps form a S–N trending arc from the Maritime Alps, close to the Mediterranean Sea, to the Pennine (Valais) Alps. On the Italian side the fore-Alpine belt is lacking, so the resulting topographic gradient is steep from the major Alpine massifs and the continental divide down to the Po Plain. Despite the high elevations of the accumulation areas, on the Italian side only two valley glaciers formed piedmont lobes during the LGM: the Dora Baltea (Gianotti et al., 2015 and references therein) in Aosta Valley and the Dora Riparia (Balestro et al., 2009a) in Susa Valley. The other glaciers were confined within their catchments, as for example with the Gesso catchment in the Maritime Alps (Federici et al., 2016). On the French side, the Isère-Arc glaciers spread out from the chain forming the Lyon piedmont lobe (Coutterand et al., 2009), while to the south all glaciers terminated still within the valleys (Jorda et al., 2000; Cossart et al., 2012; Brisset et al., 2014).

The chronological elements for the last glaciation in the western sector of the Alps are poorly documented in comparison with data for the northern (Ivy-Ochs et al., 2004; Keller and Krayss, 2005; Reitner, 2007; Akçar et al., 2011; Preusser et al., 2011; Starnberger et al., 2011; Reber et al., 2014; Ivy-Ochs, 2015) and eastern sectors (Monegato et al., 2007, 2017; Ravazzi et al., 2012, 2014; Rossato et al., 2013), where radiocarbon and exposure dating chronologies are available. Hence, the present study of the Rivoli-Avigliana end-moraine system and related Susa Valley deposits fills a critical gap and is an important step towards establishing if glaciers in the Western Alps were synchronous with the other glacial systems of the chain during the LGM.

In this perspective, exposure ages from the Maritime Alps showed that the glacial culmination in the Gesso Basin took place at 23.9 ± 1.6 ka (Federici et al., 2016). This age is in excellent agreement with exposure ages of the Trana boulders (TR1 at 24.0 ± 1.5 ka and TR2 at 20.9 ± 2.1 ka), giving the maximum culmination of the LGM in this area. Radiocarbon ages available on the French side from the Durance frontal moraine system indicate an age of 21.8–20.9 cal ka bp for the Rourebeau recessional stage (Jorda et al., 2000). The maximum advance has not been dated at the Durance system. Geochemical data from Mediterranean cores located just offshore of the Maritime Alps on the French side record marked peaks in glacier-derived sediment from the Var catchment at 26–24 and 22–20 ka (Bonneau et al., 2017). The new chronology of the Rivoli-Avigliana end-moraine system, in concert with those already mentioned, points to a culmination of Western Alpine glaciers at 26–23 ka, and therefore during Greenland stadial 3 (LGM sensu Hughes and Gibbard, 2015). This agrees with chronological data available for the central and south-eastern Alps (Monegato et al., 2007, 2017; Ravazzi et al., 2012; Scapozza et al., 2014).

Concerning the withdrawal stages, the architecture of the Rivoli-Avigliana end-moraine system displays several phases of re-advance during the LGM. The loss of ice in this early stage of decay can be inferred from the boulders' elevations in the lower reach, which is around 320 m below the elevation reached during the maximum extent. The dating results are also consistent with the timing of the onset of ice decay from other foreland sites in the Alps (Reitner, 2007; Starnberger et al., 2011; Ravazzi et al., 2012, 2014; Fontana et al., 2014; Ivy-Ochs, 2015; Hippe et al., 2018) at 19–18 ka, as well the onset of ice surface lowering in the high accumulation areas determined with 10Be dating of ice-sculpted bedrock (Wirsig et al., 2016a,2016b).

According to atmospheric circulation models, indicating that the advection moved from the western Mediterranean to the central-southeastern Alps (Florineth and Schlüchter, 2000; Luetscher et al., 2015), the Western Alps were probably underfed in terms of precipitation during the LGM. In addition, ELA reconstructions (Kuhlemann et al., 2008) confirm that high-elevation accumulation areas in this part of the chain housed smaller glaciers in relation to the mean elevation of the catchments. In this perspective, the available ELA data (accumulation area ratio method) for the Italian side (Fig. 7 longitudinal profiles) indicate a slightly lower ELA to the north (1535 m a.s.l., Forno et al., 2010) in comparison with the Maritime Alps (1645 m a.s.l., Federici et al., 2016). Based on the Gesso and Dora Baltea determinations, we estimate that the ELA related to the Dora Riparia glacier was around 1600 m a.s.l. (Fig. 7 profile B). This trend of decreasing ELA from south to north is partly due to the rapid increase of the mean altitude of topography from the Maritime Alps (maximum elevation Cima dell'Argentera, 3297 m a.s.l.) to the Graian (maximum elevation Mont Blanc, 4809 m a.s.l.) and Pennine (Valais) Alps (maximum elevation Monte Rosa, 4637 m a.s.l.) (Nigrelli et al., 2015). Despite the lowering of the ELA, piedmont lobes developed only in the major catchments (Fig. 1). The ELA trend echoes the pattern of atmospheric circulation and moisture delivery from the south, which bypassed the southern sector of the Western Alps (Luetscher et al., 2015). By contrast, the French side of the Maritime Alps was fed by orographic precipitation that led to the development of larger glaciers than on the Italian side, even if they had in some cases southern aspects (Coutterand, 2011).

Conclusions

Glacier fluctuations in the European Alps are often preserved as remarkable moraine amphitheatres. Despite intense study, fundamental questions about the chronology of glacier advances especially during the last glaciation remain unresolved, especially in the western sector of the southern side of the Alps. We present 10Be exposure dates for erratic boulders from pre-LGM, LGM and LGM recessional deposits in the Rivoli-Avigliana moraine amphitheatre. In combination with new stratigraphical and geomorphological analyses we propose revision of the chronostratigraphic attributions of the Rivoli-Avigliana end-moraine system and related deposits preserved in the lower Susa Valley.

Five boulders from sites classified as pre-LGM based on morpho- and pedostratigraphic criteria yield ages that range from 27.2 ± 1.3 to 41.2 ± 1.9 ka. All lie on the valley sides at elevations higher than 1000 m a.s.l., and thus markedly higher than the reconstructed LGM ice surface. In the amphitheatre, one boulder from a moraine located kilometres beyond both the LGM moraines and the Cresta Grande moraine (pre-LGM) has an age of 26.8 ± 2.1 ka. Of these deposits, the oldest age, 41.2 ± 1.9 ka, is interpreted to be a minimum age for the associated glaciation(s).

Concerning the last major glacier advance, the obtained data point to two major steps: (i) a maximum extension at 24.0 ± 1.5 ka, which is defined by a series of frontal moraines indicating oscillations of the glacier front, and (ii) a short readvance of the glacier at 19.6 ± 0.9 ka. Age data from correlative deposits in the Rivoli-Avigliana amphitheatre and the lateral moraines of the lower Susa Valley agree well with each other. These data agree with records from the Ivrea amphitheatre and the Gesso Valley, suggesting synchronous phases for LGM glaciers in the south-western Alps. In light of the available dataset in the Western Alps the LGM ELA for the Susa Valley is estimated to have been at about 1600 m a.s.l. for the Dora Riparia glacier.

Acknowledgements

Magali Delmas, an anonymous reviewer and editor Joe Licciardi are thanked for their thorough reviews, which greatly improved the manuscript. A portion of this work was performed in the framework of Swiss National Science Foundation projects 105220 (C. Schlüchter) and 175794 (S. Ivy-Ochs). We thank all members of Ion Beam Physics ETH Zurich for partial support of fieldwork, labwork and AMS measurements.

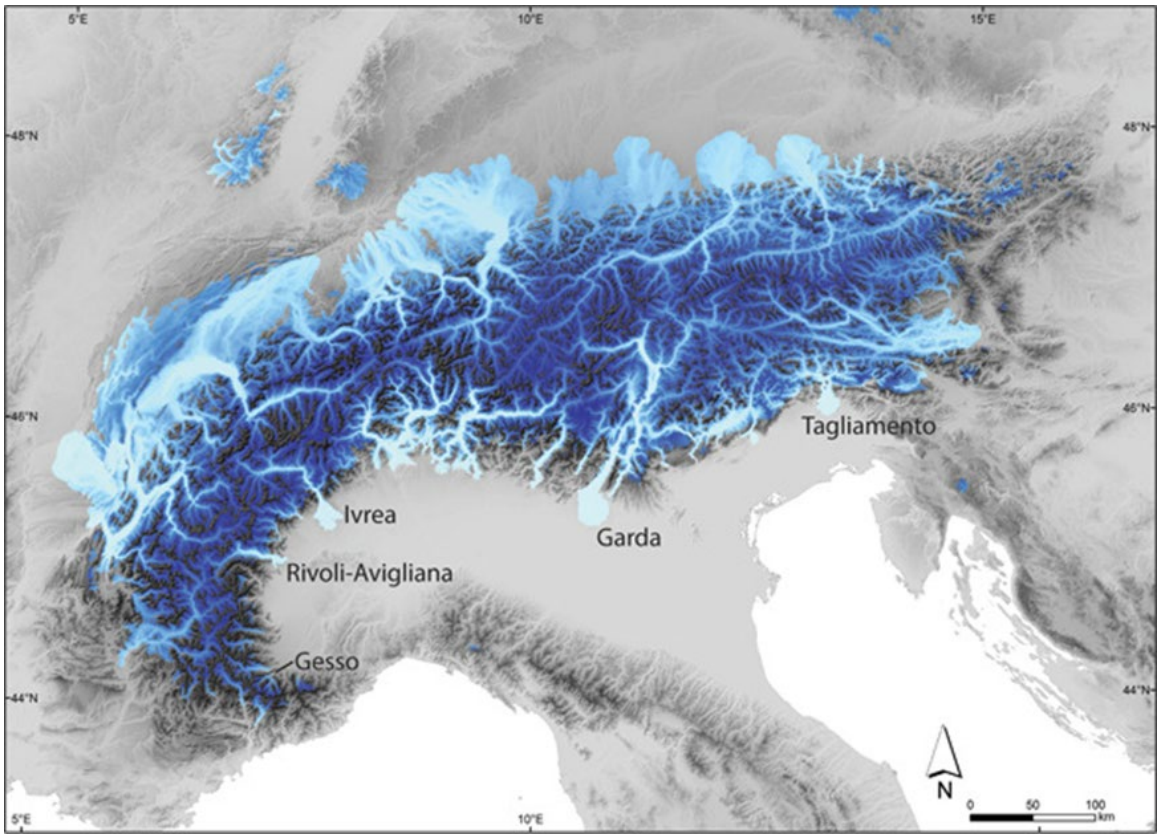

Figure1

Location of the Rivoli-Avigliana amphitheatre in the framework of maximum ice margins in the Alps during the LGM (modified from Ivy-Ochs, 2015). LGM extent is based on compilation of Ehlers and Gibbard (2004). Extents at Gesso (Federici et al., 2016), Ivrea (Gianotti et al., 2015) and Garda (Monegato et al., 2017) have been updated. Moraine amphitheatres discussed in the text are labelled.

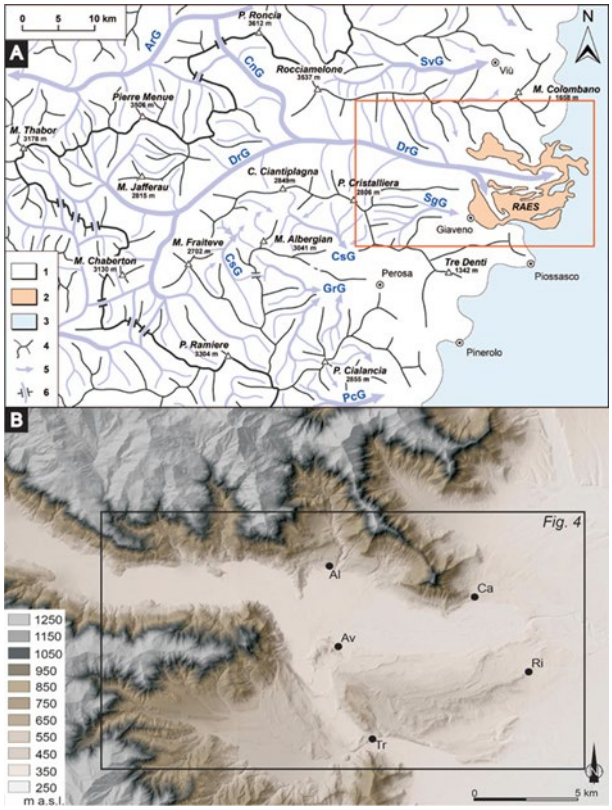

Figure2

(A) Regional scheme of the ice flow patterns in the northern Cottian Alps. (1) Undifferentiated bedrock. (2) Rivoli-Avigliana end-moraine system. (3) Alluvial Po Plain. (4) Drainage divide. (5) Ice-flow direction. (6) Glacial diffluence. ArG: Arc Glacier; CnG: Cenischia Glacier; CsG: Chisone Glacier; DrG: Dora Riparia Glacier; GrG: Germanasca Glacier; PcG: Pellice Glacier. SvG: Stura di Viù Glacier; SgG: Sangone Glacier. (B) Colour shaded relief digital elevation model of the lower Susa Valley. The Cresta Grande moraine extends to the west-southwest from the point marked Ri. At the point marked Tr the outermost LGM moraines are evident. Al: Almese; Av: Avigliana; Ca: Caselette; Ri: Rivoli Torinese; Tr: Trana. Area covered in Fig. 4 is shown.

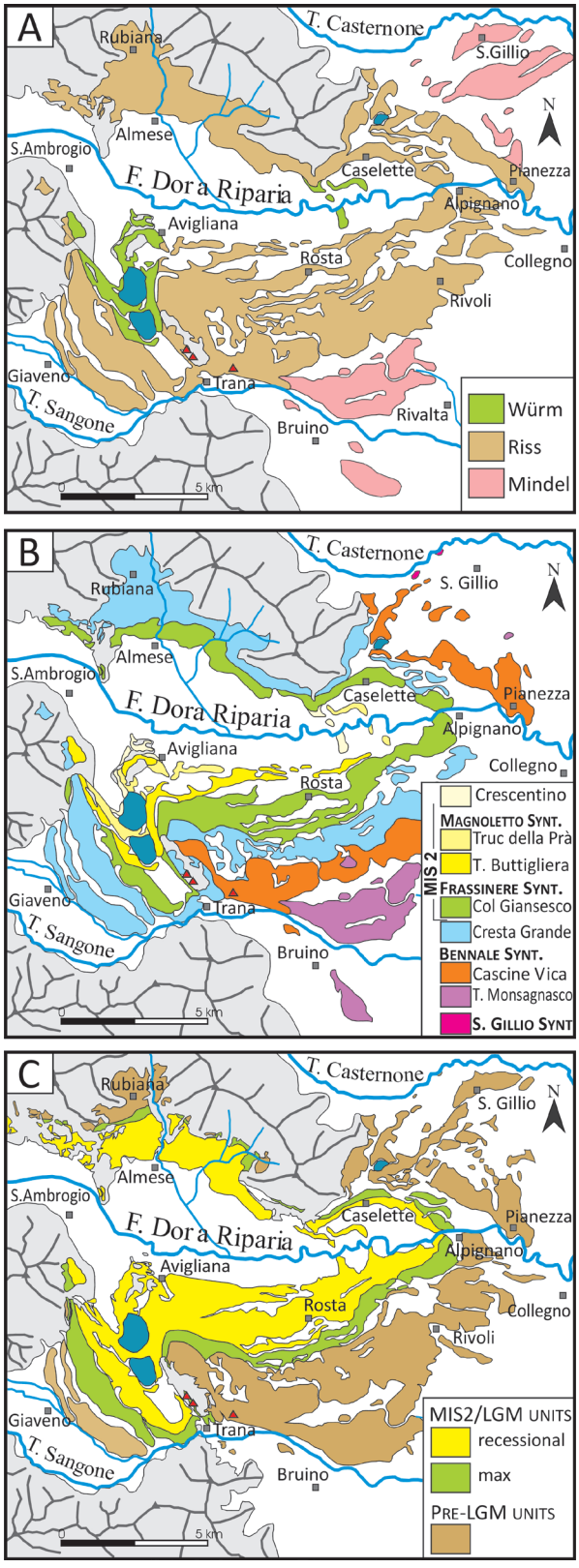

Figure3

Three interpretations for the age attribution of the Rivoli-Avigliana amphitheatre moraines: (A) Petrucci (1970) referring to the glaciations of Penck and Brückner (1909) (Mindel, Riss, Würm); (B) based on Geological Map of Italy at 1: 50 000 scale (Balestro et al., 2009a); and (C) this work. Note the striking difference of the location of the LGM moraines (green) in the three maps, especially on the right lateral side near the two lakes. Locations of dated amphitheatre boulders are shown as red triangles.

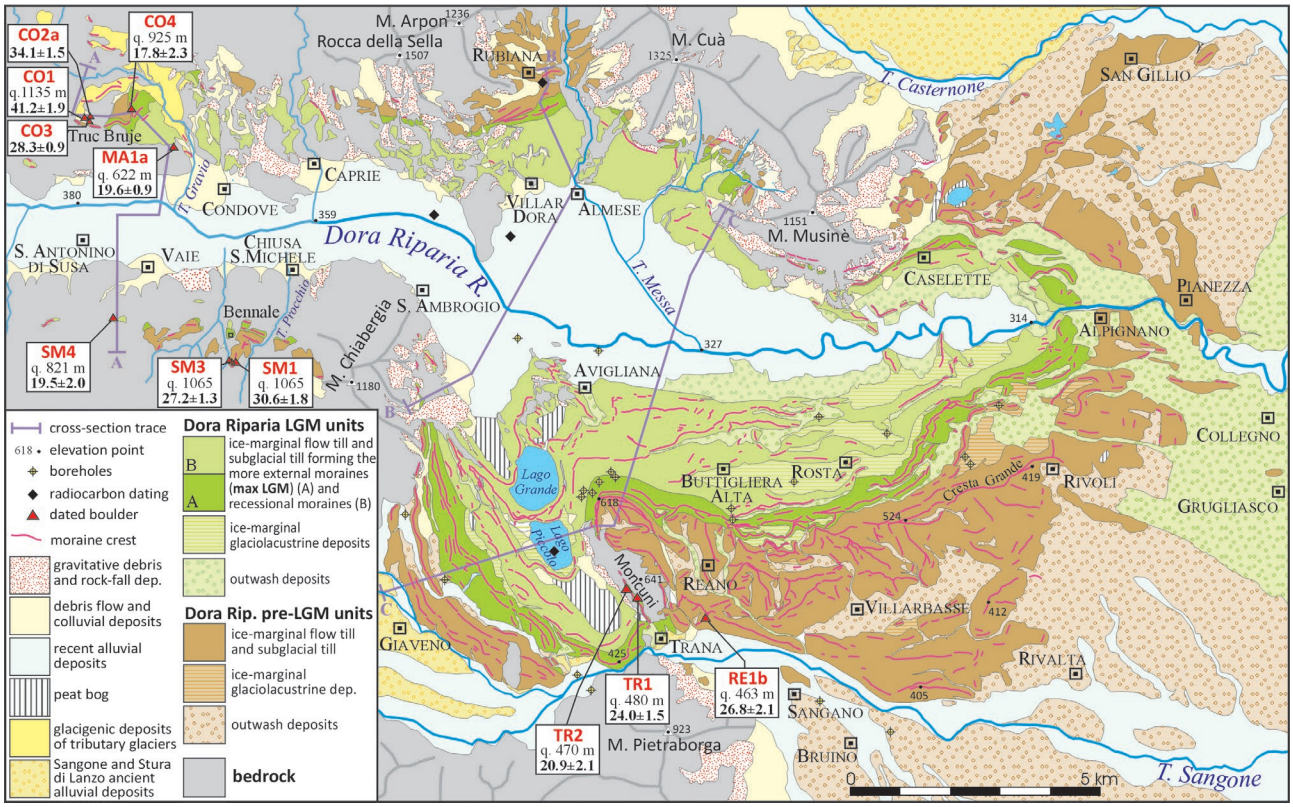

Figure4

Geological map of the Rivoli-Avigliana end-moraine system. The glacial succession of the Dora Riparia glacier is summarized into three groups: pre-LGM units, maximum LGM units and recessional LGM units. The sampled erratic boulders with their exposure ages are highlighted (white boxes). The traces of the cross-sections of Fig. 6 are shown.

Label	Size L × H × W (m)	Lithology	Latitude (°N)	Longitude (°E)	Elevation (m a.s.l.)	Thickness (cm)	Shielding	^{10}Be (10^4 atoms/g)	Exposure age (a)	Unit attribution*
MA1a	2.5 × 3.5 × 3	Gneiss	45.2086	7.5008	622	4	0.949	12.125 ± 0.535	19 630 ± 880	LGM withdrawal (L)
SM4	15 × 8 × 10	Granite	45.1578	7.4706	821	4	0.994	14.845 ± 1.484	19 500 ± 1990	LGM withdrawal (R)
CO4	5 × 12 × 4	Gneiss	45.2167	7.4794	925	4	0.977	14.561 ± 1.907	17 840 ± 2390	LGM maximum position (L)
TR1	4 × 5 × 3	Gneiss	45.0803	7.6914	480	3	0.994	13.798 ± 0.811	24 030 ± 1450	LGM maximum position (A)
TR2	8 × 6 × 10	Gneiss	45.0833	7.6833	470	2	0.994	12.036 ± 1.180	20 900 ± 2100	LGM maximum position (A)
RE1b	7 × 5 × 3	Gneiss	45.0731	7.7272	463	2	1.000	15.334 ± 1.163	26 800 ± 2090	Pre-LGM (A)
SM1	4 × 5 × 2.5	Gneiss	45.1483	7.5208	1065	4	0.982	27.640 ± 1.540	30 560 ± 1760	Pre-LGM (R)
SM3	2.2 × 2.5 × 2.2	Quartzite	45.1486	7.5197	1065	4	0.997	25.064 ± 1.167	27 210 ± 1310	Pre-LGM (R)
CO1	3 × 3.5 × 2	Gneiss	45.2219	7.4575	1135	4	1.000	39.641 ± 1.766	41 170 ± 1920	Pre-LGM (L)
CO2a	2 × 2 × 2	Quartzite	45.2219	7.4608	1133	4	0.892	29.530 ± 1.274	34 070 ± 1520	Pre-LGM (L)
CO3a	2 × 2 × 1.5	Gneiss	45.2214	7.4611	1130	4	0.834	23.681 ± 1.226	29 080 ± 1560	Pre-LGM (L)
CO3b	2 × 2 × 1.5	Gneiss	45.2214	7.4611	1130	4	0.834	22.755 ± 0.876	27 910 ± 1110	Pre-LGM (L)

Table 1.

Rivoli-Avigliana amphitheatre and lower Susa Valley erratic boulder 10Be data; site, lithology, AMS results and calculated ages, as well as chronostratigraphic attribution are given

* L, left side; R, right side, A, amphitheatre.

AMS measurement errors are at 1σ level, including the statistical (counting) error and the error due to normalization to standards (07KNSTD) and blanks.

Ages are calculated with the NE North America (NENA) spallation production rate at sea level and high latitude of 3.93 ± 0.19 10Be atom g quartz−1 a−1 (Balco et al., 2009), with 'St' scaling.

Figure5

Photos of sampled boulders. In the Susa Valley: (A) CO1, (B) CO2a, (C) SM1, (D) CO4, (E) SM4. In the amphitheatre: (F) RE1b, (G) TR1, (H) TR2 and (I) detail of TR2. See Fig. 4 for boulder locations and 10Be dates.

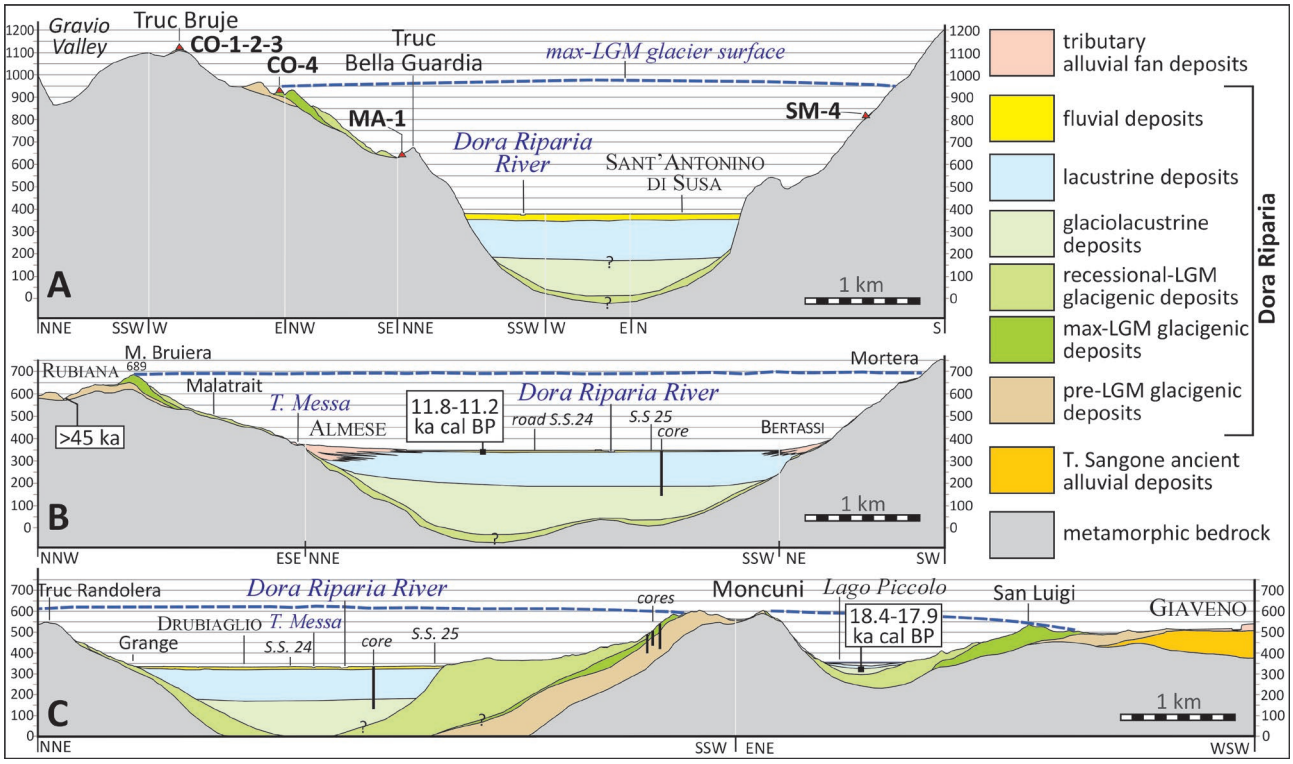

Figure6

Cross-sections of the lower Susa Valley and the Rivoli-Avigliana end-moraine system (trace locations in Fig. 4). The radiocarbon dates from the Rubiana moraine (this work) and from the internal alluvial plain (Charrier and Peretti, 1973, Charrier and Peretti, 1975) and from Lago Piccolo (Finsinger et al., 2006; Larocque and Finsinger, 2008) are shown in cross-sections B and C, respectively.

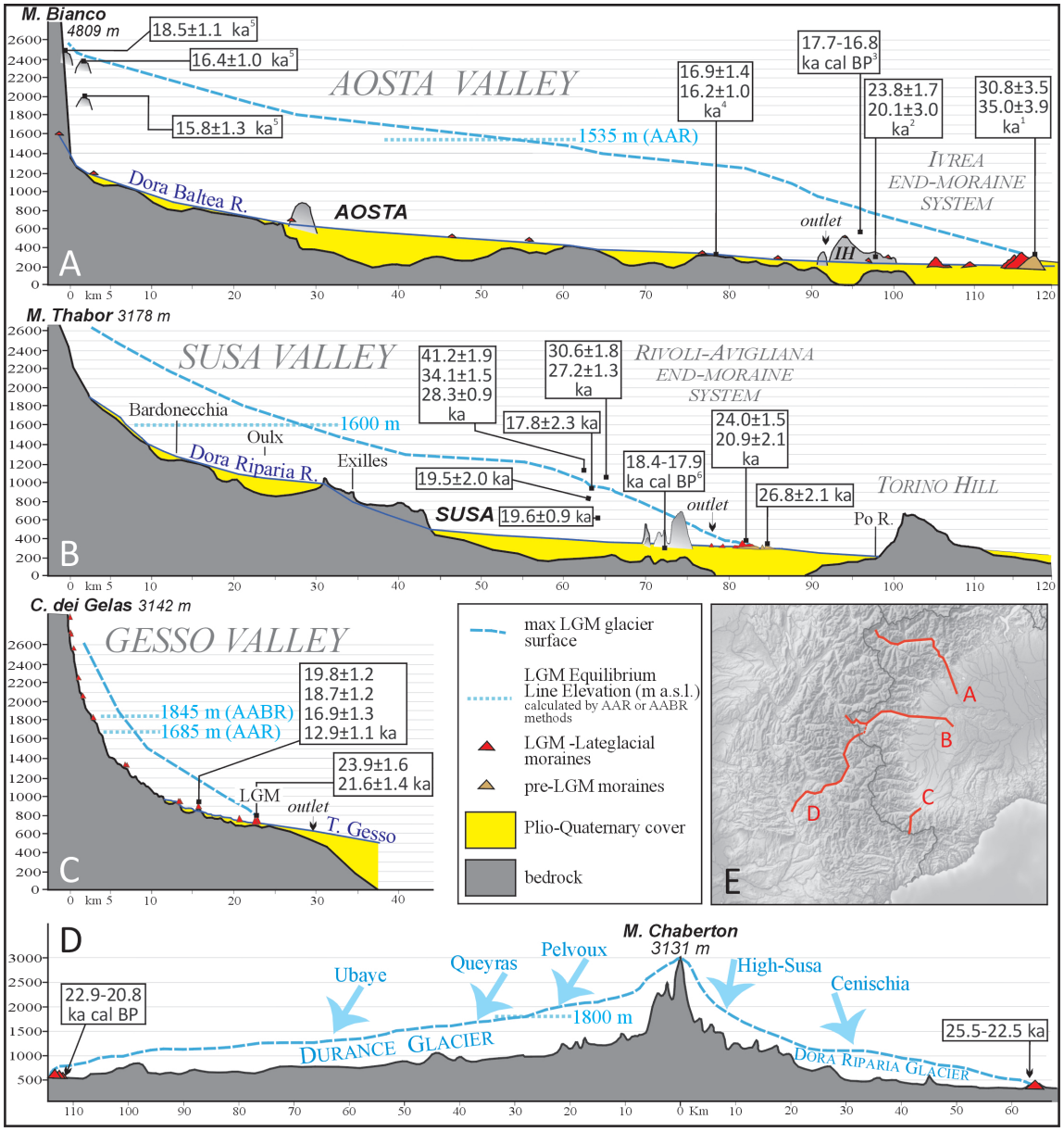

Figure7

Longitudinal profiles of the Aosta, Susa, Gesso (on the Italian side of the Alpine range) and Durance Valleys (on the French side) and their end-moraine systems, with the reconstructed LGM glacier extents. All exposure ages are calculated in the same manner as in this work. Previous and new exposure and radiocarbon ages are reported. In the Dora Baltea basin (A) they are: erratics on the pre-LGM External Serra moraine (1), erratics on Ivrea bedrock hills (IH) (2) and the roche moutonnée at Donnas (4) (Gianotti et al., 2008, 2015); Alice Superiore peat bog (3) (Schneider, 1978); polished bedrock surfaces at Aiguille du Châtelet (2488 m), Testa Bernarda (2402 m a.s.l.) and M. La Saxe (1913–2017 m a.s.l.) (5) (Wirsig et al., 2016a). In the Dora Riparia basin (B) all data come from this work, apart from the radiocarbon dating from Lago Piccolo (Finsinger et al., 2006; Larocque and Finsinger, 2008) (6). In the Gesso basin (C) the dates are referred to the LGM and the early Lateglacial stadial (Federici et al., 2012, Federici et al., 2016). ELA position during the LGM in the Susa Valley is estimated at an intermediate elevation between the ELAs for the Gesso Valley (Federici et al., 2016) and the lower Aosta Valley (Forno et al., 2010). In the Durance basin (D) the radiocarbon results date an LGM recessional stage (Jorda et al., 2000).

References

- Akçar N, Ivy-Ochs S, Kubik PW et al. 2011. Post-depositional impacts on 'Findlinge' (erratic boulders) and their implications for surface-exposure dating. Swiss Journal of Geosciences 104: 445– 453.
- Balco G, Briner J, Finkel RC et al. 2009. Regional beryllium-10 production rate calibration for late-glacial northeastern North America. Quaternary Geochronology 4: 93– 107.
- Balco G, Stone JO, Lifton NA et al. 2008. A complete and easily accessible means of calculating surface exposure ages or erosion rates from 10Be and 26Al measurements. Quaternary Geochronology 3: 174– 195.
- Balestro G, Cadoppi P, Perrone G et al. 2009b. Tectonic evolution along the Col del Lis-Trana deformation Zone (Internal Western Alps). Italian Journal of Geoscience 128: 331– 339.
- Balestro G, Cadoppi P, Piccardo GB et al. 2009a. Note illustrative della Carta Geologica d'Italia alla scala 1:50.000: Foglio 155 Torino Ovest. ISPRA-Servizio Geologico d'Italia − ARPA Piemonte.
- Barféty JC, Lemoine M, Graciansky PCD et al. 1996 Carte géologique de France (1/50 000), Feuille Briançon. BRGM: Orléans, France.
- Bini A. 1997. Problems and methodologies in the study of the Quaternary deposits of the Southern side of the Alps. Geologia Insubrica 2: 11– 20.
- Bonneau L, Toucanne S, Bayon G et al 2017. Glacial erosion dynamics in a small mountainous watershed (Southern French Alps): A source-to-sink approach. Earth and Planetary Science Letters 458: 366– 379.
- Bonsignore G, Bortolami GC, Elter G et al. 1969. Note Illustrative della Carta Geologica d'Italia alla scala 1:100.000: Fogli 56 e 57 "Torino" e "Vercelli", 2a ed. Servizio Geologico d'Italia.
- Borchers B, Marrero S, Balco G et al. 2016. Geological calibration of spallation production rates in the CRONUS-Earth project. Quaternary Geochronology 31: 188– 198.
- Brisset E, Miramont C, Guiter F et al. 2014. A new contribution to the chronology of the deglaciation in the upper Verdon valley (lake Allos, Southern French Alps). Quaternaire 25: 147– 156.
- Cadoppi P, Castelletto M, Sacchi R et al. 2002. Note illustrative della Carta Geologica d'Italia alla scala 1:50.000: Foglio 154 Susa. ISPRA-Servizio Geologico d'Italia − ARPA Piemonte 154.
- Carraro F, Cadoppi P, Baggio P et al. 2002. Susa − 154 sheet, Geological Map of Italy, 1:50.000 scale. APAT: Rome, Italy.
- Carraro F, Lanza R, Perotto A et al. 1991. L'evoluzione morfologica del Biellese occidentale durante il Pliestocene inferiore e medio, in relazione all'inizio della costruzione dell 'Anfiteatro Morenico d'Ivrea. Bollettino Museo Regionale di Scienze Naturali Torino 9: 99– 117.
- Champagnac JD, Molnar P, Anderson RS et al. 2007. Quaternary erosion-induced isostatic rebound in the western Alps. Geology 35: 195– 198.
- Charrier G, Peretti L. 1973. Ricerche sull'evoluzione del clima e dell'ambiente durante il Quaternario nel settore delle Alpi occidentali italiane: IV. Tardoglaciale e Finiglaciale di Villar Dora nella bassa valle della Dora Riparia. Allionia 19: 97– 143.
- Charrier G, Peretti L. 1975. Analisi palinologica e datazione radiometrica C14 di depositi torbosi intermorenici della regione alpina piemontese, applicate allo studio del clima e dell'ambiente durante il Quaternario superiore. Bollettino Comitato Glaciologico Italiano 23: 51– 66.
- Christl M, Vockenhuber C, Kubik PW et al. 2013. The ETH Zurich AMS facilities: performance parameters and reference materials. Nuclear Instruments and Methods in Physics Research Section B: Beam Interactions with Materials and Atoms 294: 29– 38.
- Clark PU, Dyke AS, Shakun JD et al. 2009. The Last Glacial Maximum. Science 325: 710– 714.
- Claude A, Ivy-Ochs S, Kober F et al. 2014. The Chironico landslide (Valle Leventina, southern Swiss Alps): age and evolution. Swiss Journal of Geosciences 107: 273– 291.

- Cossart E, Fort M, Bourlès D et al. 2012. Deglaciation pattern during the Lateglacial/Holocene transition in the southern French Alps. Chronological data and geographical reconstruction from the Clarée Valley (upper Durance catchment, southeastern France). Palaeogeography, Palaeoclimatology, Palaeoecology 315–316: 109– 123.
- Coutterand S. 2011. Les Alpes Occidentales au Dernier Maximum Glaciaire (LGM). Available at: www.glaciers-climat.com.
- Coutterand S, Schoeneich P, Nicoud G. 2009. Le lobe glaciaire lyonnais au maximum würmien: glacier du Rhône ou/et glaciers savoyard? Neige et glace de montagne, reconstitution, dynamique, pratiques. Collection EDYTEM, Cahiers de Géographie 8: 11– 22.
- Delmas M. 2015. The last maximum ice extent and subsequent deglaciation of the Pyrenees: an overview of recent research. Cuadernos de Investigación Geográfica 41: 359– 387.
- Ehlers J, Gibbard PL. 2004 Quaternary Glaciations-Extent and Chronology: Part I: Europe. Elsevier: Amsterdam.
- Federici PR, Granger DE, Ribolini A et al. 2012. Last glacial maximum and the Gschnitz stadial in the maritime Alps according to 10Be cosmogenic dating. Boreas 41: 277– 291.
- Federici PR, Ribolini A, Spagnolo M. 2016. The glacial history of the maritime Alps from the last glacial maximum to the little ice age. Geological Society of London Special Publications 433: SP433– SP439.
- Finsinger W, Tinner W, Vanderknaap WO et al. 2006. The expansion of hazel (Corylus avellana L.) in the southern Alps: a key for understanding its Early Holocene history in Europe? Quaternary Science Reviews 25: 612– 631.
- Florineth D, Schlüchter C. 2000. Alpine evidence for atmospheric circulation patterns in Europe during the last glacial maximum. Quaternary Research 54: 295– 308.
- Fontana A, Monegato G, Zavagno E et al. 2014. Evolution of an alpine fluvioglacial system at the LGM decay: the Cormor megafan (NE Italy). Geomorphology 204: 136– 153.
- Forno MG, Gianotti F, Racca G. 2010. Significato paleoclimatico dei rapporti tra il glacialismo principale e quello tributario nella bassa valle della Dora Baltea. Quaternario 23: 105– 124.
- Franchi S, Mattirolo O, Novarese V et al. 1925. Foglio 56 “Torino” della Carta al 100.000 dell'Istituto Geografico Militare. Regio Ufficio Geologico Italiano.
- Galadini F, Poli ME, Zanferrari A. 2005. Seismogenic sources potentially responsible for earthquakes with M≥ 6 in the eastern Southern Alps (Thiene-Udine sector, NE Italy). Geophysical Journal International 161: 739– 762.
- Gastaldi B. 1872. Cenni sulla costituzione geologica del Piemonte. Bollettino Regio Comitato Geologico Italiano 3: 14– 32.
- Gianotti F, Forno MG, Ivy-Ochs S et al. 2008. New chronological and stratigraphical data on the Ivrea amphitheatre (Piedmont, NW Italy). Quaternary International 190: 123– 135.
- Gianotti F, Forno MG, Ivy-Ochs S et al. 2015. Stratigraphy of the Ivrea morainic amphitheatre (NW Italy): an updated synthesis. Alpine and Mediterranean Quaternary 28: 29– 58.
- Gibbons AB, Megeath JD, Pierce KL. 1984. Probability of moraine survival in a succession of glacial advances. Geology 12: 327– 330.
- Graf AA. 2008. Surface exposure dating on LGM and pre-LGM erratic boulders − A comparison of paleoclimate records from both hemispheres. PhD Dissertation, University of Bern.
- Graf A, Akçar N, Ivy-Ochs S et al. 2015. Multiple advances of alpine glaciers into the Jura Mountains in the northwestern Switzerland. Swiss Journal of Geosciences 108: 225– 238.
- Heyman J. 2014. Paleoglaciation of the Tibetan Plateau and surrounding mountains based on exposure ages and ELA depression estimates. Quaternary Science Reviews 91: 30– 41.

- Hippe K, Fontana A, Hajdas I et al. 2018. A high-resolution 14C chronology tracks pulses of aggradation of glaciofluvial sediment on the Cormor megafan between 45 and 20 ka BP. Radiocarbon DOI 10.1017/RDC.2018.21.
- Hofer D, Raible CC, Dehnert A et al. 2012. The impact of different glacial boundary conditions on atmospheric dynamics and precipitation in the North Atlantic region. Climate of the Past 8: 935– 949.
- Hughes PD, Gibbard PL. 2015. A stratigraphical basis for the last glacial maximum (LGM). Quaternary International 383: 174– 185.
- Ivy-Ochs S. 2015. Glacier variations in the European Alps at the end of the last glaciation. Cuadernos de Investigación Geográfica 41: 295– 315.
- Ivy-Ochs S, Kerschner H, Reuther A et al. 2006. The timing of glacier advances in the northern European Alps based on surface exposure dating with cosmogenic 10Be, 26Al, 36Cl and 21Ne. Geological Society of America Special Papers 415: 43– 60.
- Ivy-Ochs S, Schäfer J, Kubik PW et al. 2004. Timing of deglaciation on the northern Alpine foreland (Switzerland). Eclogae Geologicae Helvetiae 97: 47– 55.
- Jorda M, Rosique T, Évin J. 2000. Données nouvelles sur l'age du dernier maximum glaciaire dans les Alpes méridionales françaises. Comptes Rendus de l'Académie des Sciences − Series IIA − Earth and Planetary Science 331: 187– 193.
- Keller O, Krayss E. 2005. Der Rhein-Linth Gletscher im Letzten Hochglazial. 2. Teil: Datierung und Modelle der Rhein-Linth-Vergletscherung, Klimarekonstruktionen. Vierteljahresschrift der Naturforschenden Gesellschaft in Zürich 150: 69– 85.
- Kuhlemann J, Rohling EJ, Krumrei I et al. 2008. Regional synthesis of Mediterranean atmospheric circulation during the Last Glacial Maximum. Science 321: 1338– 1340.
- Lambeck K, Rouby H, Purcell A et al. 2014. Sea level and global ice volumes from the last glacial maximum to the Holocene. Proceedings of the National Academy of Sciences USA 111: 15296– 15303.
- Larocque I, Finsinger W. 2008. Late-glacial chironomid-based temperature reconstructions for Lago Piccolo di Avigliana in the southwestern Alps (Italy). Palaeogeography, Palaeoclimatology, Palaeoecology 257: 207– 223.
- Ludwig P, Schaffernicht EJ, Shao Y et al. 2016. Regional atmospheric circulation over Europe during the Last Glacial Maximum and its links to precipitation. Journal of Geophysical Research: Atmospheres 121: 2130– 2145.
- Luetscher M, Boch R, Sodemann H et al. 2015. North Atlantic storm track changes during the last glacial maximum recorded by alpine speleothems. Nature Communications 6: 6344.
- Mattirolo E, Novarese V, Franchi S et al. 1910. Carta Geologica d'Italia alla scala 1:100.000, Foglio 55 “Susa”. 1a ed. Servizio Geologico d'Italia.
- Mey J, Scherler D, Wickert AD et al. 2016. Glacial isostatic uplift of the European Alps. Nature Communications 7: 13382.
- Monegato G. 2012. Local glaciers in the Julian Prealps (NE Italy) during the Last Glacial Maximum. Alpine and Mediterranean Quaternary 25: 5– 14.
- Monegato G, Ravazzi C, Donegana M et al. 2007. Evidence of a 2-fold glacial advance during the last glacial maximum in the Tagliamento end moraine system (Eastern Alps). Quaternary Research 68: 284– 302.
- Monegato G, Scardia G, Hajdas I et al. 2017. The Alpine LGM in the boreal ice-sheets game. Scientific Reports 7: 2078.
- Nigrelli G, Lucchesi S, Bertotto S et al. 2015. Climate variability and Alpine glaciers evolution in Northwestern Italy from the Little Ice Age to the 2010s. Theoretical and Applied Climatology 122: 595– 608.

- Nishiizumi K, Imamura M, Caffee MW et al. 2007. Absolute calibration of 10Be AMS standards. Nuclear Instruments and Methods in Physics Research Section B: Beam Interactions with Materials and Atoms 258: 403– 413.
- Nocquet JM, Sue C, Walpersdorf A et al. 2016. Present-day uplift of the western Alps. Scientific Reports 6: 28404.
- Penck A, Brückner E. 1909. Die Alpen im Eiszeitalter. Tauchnitz: Leipzig.
- Perrone G, Cadoppi P, Tallone S. 2015. Geometry and impact of transpressional faulting in polyphasic metamorphic orogenic belts: the Viù Deformation Zone (inner Western Alps). International Geology Review 57: 1889– 1921.
- Perrone G, Eva E, Solarino S et al. 2010. Seismotectonic investigations in the inner Cottian Alps (Italian Western Alps): an integrated approach. Tectonophysics 496: 1– 16.
- Petrucci F. 1970. Rilevamento geomorfologico dell'Anfiteatro morenico di Rivoli-Avigliana. Memorie della Societá Italiana di Scienze Naturali 18: 95– 124.
- Polino R, Dela Pierre F, Borghi A et al. 2002. Note Illustrative della Carta Geologica d'Italia alla scala 1:50.000–Foglio 153 'Bardonecchia'. Servizio Geologico d'Italia.
- Preusser F, Graf HR, Keller O. 2011. Quaternary glaciation history of northern Switzerland. Quaternary Science Journal 60: 282– 305.
- Ravazzi C, Badino F, Marsetti D et al. 2012. Glacial to paraglacial history and forest recovery in the Oglio glacier system (Italian Alps) between 26 and 15 ka cal bp. Quaternary Science Reviews 58: 146– 161.
- Ravazzi C, Pini R, Badino F et al. 2014. The latest LGM culmination of the Garda Glacier (Italian Alps) and the onset of glacial termination. Age of glacial collapse and vegetation chronosequence. Quaternary Science Reviews 105: 26– 47.
- Reber R, Akçar N, Ivy-Ochs S et al. 2014. Timing of retreat of the Reuss glacier (Switzerland) at the end of the last glacial maximum. Swiss Journal of Geosciences 107: 293– 307.
- Reitner JM. 2007. Glacial dynamics at the beginning of Termination I in the Eastern Alps and their stratigraphic implications. Quaternary International 164–165: 64– 84.
- Rose J, Menzies J. 1996. Glacial stratigraphy. In Past Glacial Environments: Glacial Environments: Sediments, Forms and Techniques, J Menzies (ed.). Butterworth-Heinemann: Oxford 253– 284.
- Rossato S, Monegato G, Mozzi P et al. 2013. Late Quaternary glaciations and connections to the Piedmont plain in the Prealpine environment: the middle and lower Astico Valley (NE Italy). Quaternary International 288: 8– 24.
- Sacco F. 1887. L'anfiteatro morenico di Rivoli. Bollettino Regio Comitato Geologico 18: 141– 180.
- Scapozza C, Castelletti C, Soma L et al. 2014. Timing of LGM and deglaciation in the Southern Swiss Alps. Géomorphologie: Relief, Processus, Environnement 20: 307– 322.
- Scardia G, De Franco R, Muttoni G et al. 2012. Stratigraphic evidence of a Middle Pleistocene climate-driven flexural uplift in the Alps. Tectonics 31, TC6004.
- Scardia G, Festa A, Monegato G et al. 2015. Evidence for late Alpine tectonics in the Lake Garda area (Northern Italy) and seismogenic implications. Geological Society of America Bulletin 127: 113– 130.
- Schneider RE. 1978. Pollenanalytische Untersuchungen zur Kenntnis der Spät-und postglazialen Vegetationsgeschischte am Südrand der Alpen zwischen Turin und Varese (Italien). Botanische Jahrbücher für Systematik, Pflanzengeschichte und Pflanzengeographie 100: 26– 109.
- Shakun JD, Carlson AE. 2010. A global perspective on Last Glacial Maximum to Holocene climate change. Quaternary Science Reviews 29: 1801– 1816.
- Starnberger R, Rodnight H, Spötl C. 2011. Chronology of the last glacial maximum in the Salzach palaeoglacier area (Eastern Alps). Journal of Quaternary Science 26: 502– 510.

- Sternai P, Herman F, Champagnac J-D et al. 2012. Pre-glacial topography of the European Alps. Geology 40: 1067– 1070.
- Stone JO. 2000. Air pressure and cosmogenic isotope production. Journal of Geophysical Research: Solid Earth 105: 23753– 23759.
- Sue C, Tricart P. 2003. Neogene to current normal faulting in the inner Western Alps: A major evolution of the late alpine tectonics. Tectonics 22: 1050.
- Wirsig C, Zasadni J, Christl M et al. 2016a. Dating the onset of LGM ice surface lowering in the High Alps. Quaternary Science Reviews 143: 37– 50.
- Wirsig C, Zasadni J, Ivy-Ochs S et al. 2016b. A deglaciation model of the Oberhasli, Switzerland. Journal of Quaternary Science 31: 46– 59.